Research Paper
Computational Methods for Differential Equations
http://cmde.tabrizu.ac.ir
Vol. 14, No. 1, 2026, pp. 110-128
DOI:10.22034/cmde.2024.64161.2891

Numerical solution of stochastic fractional integro-differential and Itô-Volterra integral equations via fractional Genocchi wavelets

Parisa Rahimkhani[1], Yadollah Ordokhani[2,*], and Pedro M Lima[3]

[1]Faculty of Science, Mahallat Institute of Higher Education, Mahallat, Iran.

[2]Department of Mathematics, Faculty of Mathematical Sciences, Alzahra University, Tehran, Iran.

[3]Centro de Matemática Computacional e Estocástica, Instituto Superior Téecnico, Universidade de Lisboa, Portugal.

Abstract

In this research, a novel approach based on the fractional-order Genocchi wavelets (FGWs), inverse hyperbolic functions, and collocation technique is introduced for obtaining numerical solutions of stochastic fractional integro-differential equations (SFIDEs) and Itô-Volterra integral equations (IVIEs). Initially, we utilize the Laplace transform approach to approximate the Caputo fractional derivative. Then, the unknown solution is approximated via a combination of the FGWs and inverse hyperbolic functions. We replace this approximation and its derivatives in the resulting stochastic equation (SE). By the Gauss-Legendre quadrature rule (GLQR) and collocation method, we obtain a system of nonlinear algebraic equations. The derived algebraic system can be readily solved through application of Newton's iterative scheme. Also, we show the convergence of the mentioned scheme. Ultimately, several test problems are examined to demonstrate the applicability and effectiveness of the suggested technique.

Keywords. Fractional-order Genocchi wavelets, Fractional stochastic integro-differential equations, Laplace transform, Convergence analysis.
2010 Mathematics Subject Classification. 65C30, 65L60, 34A08.

1. Introduction

The theory of fractional integration and differentiation is applicable across various fields. In particular, fractional integro-differential equations (FIDEs) have been found useful in rheology, viscoelasticity, porous media, and fluid dynamics ([9, 10, 18, 26]). As obtaining exact solutions for most FIDEs is difficult, developing numerical methods for their approximation is essential. Various methods have been proposed, including fractional-order Bernoulli functions [34], fractional alternative Legendre functions [31], shifted Legendre polynomials operational matrix [11], Jacobi polynomials Galerkin and collocation [41], Homotopy analysis [44], Bessel functions [27], Bell polynomials [28], wavelets neural networks [30], Müntz-Legendre polynomials and Petrov-Galerkin [38], and spectral [40] method.

SEs are extensively used to model problems in engineering, medical, biology, physical, and finance ([1], [4]). For instance, SEs may be found in the stochastic representation of reactor dynamics problems [5], and the dynamics of biological population growth [17]. Due to the existence of a noise source, such as Gaussian white noise, finding an analytical solution for SEs is often very challenging, or even impossible. Thus, introducing some numerical techniques for finding approximate solutions of these problems is an essential requirement. Many researchers developed different numerical techniques to solve various types of SEs such as Chebyshev wavelets [23], delta functions [20], Taylor series [15], generalized hat basis functions [12], triangular functions [16], Bernstein polynomials [21], Euler polynomials [22], fractional-order Genocchi deep neural networks [29], Euler-Maruyama and Milstein's [14] method.

A SFIDE is characterized by a non-integer order derivative within the framework of a stochastic integro-differential equation. Due to the application of SFIDEs to model real phenomena involving memory and hereditary properties, there is a strong inclination to seek approximate solutions for these equations. So, SFIDEs have solved by various

Received: 24 October 2024; Accepted: 20 January 2025.
∗ Corresponding author. Email: ordokhani@alzahra.ac.ir.

numerical techniques such as spectral collocation [43], Monte-Carlo Galerkin [3], block pulse [2], and wavelets Galerkin [24] method.

Recently, different orthogonal functions or polynomials were applied to estimate numerical solution of various equations, for example, Walsh functions, block pulse functions, Fourier series, Legendre polynomials, Chebyshev polynomials, Laguerre polynomials and wavelets.

Wavelets analysis has garnered acclaim across various scientific disciplines due to its effective applications in image processing, signal processing, computational mathematics, and time-frequency analysis. Key properties of wavelets include: arbitrary regularity, characteristics orthogonality, good localization and wavelets serve as an unconditional (Riesz) basis for $L^2(R)$, signifying that any function within $L^2(R)$ can be both decomposed and reconstructed using wavelets ([6, 19]). Various techniques based on wavelets were extended for solving different fractional and integer order integro-differential equations. For example, the Bernoulli wavelets approach has been utilized to solve fractional delay differential equations [33], the Müntz-Legendre wavelets approach has been used to determine the numerical solution of fractional-order integration [35], the Fibonacci wavelets method has been applied for the numerical solution of fractional optimal control problems [39], the Chelyshkov wavelets method has been introduced to solve distributed-order fractional differential equations [36], the Bernstein wavelets method has been employed to estimate the numerical solution of distributed-order fractional optimal control problems [32], etc.

The Genocchi wavelets have many useful properties over an interval. We can deduce these properties from the Genocchi polynomials properties, such as [7]

- The coefficients of the individual terms in the Genocchi polynomials are integers. Thus, there is no computational error, unlike most polynomials where the coefficients of individual terms are not integers, such as in the case of Legendre and Bernoulli polynomials. This property demonstrates the superiority of Genocchi polynomials over Bernoulli polynomials.
- The Genocchi polynomials consist of fewer terms compared to other polynomials. For instance the Genocchi polynomial $G_6(t)$ has 4 terms, while the Bernoulli polynomial $B_6(t)$ has 5 terms, and both the shifted Chebyshev $T_6(t)$ and shifted Legendre polynomial $L_6(t)$ have 7 terms. Therefore, when approximating an arbitrary function, the Genocchi polynomials require less CPU time compared to the Bernoulli, shifted Chebyshev, and shifted Legendre polynomials.

Also, a simple code written in Mathematica or Maple can be applied to obtain all the Genocchi wavelets of any order m over interval $[\frac{n-1}{2^{k-1}}, \frac{n}{2^{k-1}})$.

1.1. **The main goal of this paper.** In this research, we introduce an innovative approach utilizing the FGWs and inverse hyperbolic functions to solve IVIEs and SFIDEs. To obtain the desired aim, we introduce the FGWs and their properties. Then, we present an approximation for an equivalent integro-differential equation (IDE) from the original fractional IDE by applying the Laplace transform technique. By using the FGWs, inverse hyperbolic functions, GLQR, and collocation method, we achieve a set of nonlinear algebraic equations. Some advantages of the presented scheme include:

- Straightforward computation and ease of implementation.
- The approximate solution obtained by this approach is a continuous function satisfying the initial conditions.
- Fractional-order wavelets possess three degrees of freedom.
- Satisfactory results can be achieved using a small number of FGWs basis functions.
- By converting the fractional-order integro-differential equation into an integer order one, the computational cost is significantly reduced.
- This strategy can be employed to solve systems of fractional differential equations (FDEs), fractional partial differential equations, inverse problems, etc.

1.2. **Problem statement.** We consider two classes of stochastic problems as:

Type 1:

First, we consider the following IVIEs as

$$f(\xi) = g(\xi) + \int_0^{\xi} \mathcal{K}_1(\tau, \xi, f(\tau))d\tau + \int_0^{\xi} \mathcal{K}_2(\tau, \xi, f(\tau))dB(\tau). \tag{1.1}$$

Type 2:
Second, we consider the following SFIDE:

$$D^{\gamma}f(\xi) = g(\xi) + \int_0^{\xi} \mathcal{K}_1(\tau,\xi,f(\tau))d\tau + \int_0^{\xi} \mathcal{K}_2(\tau,\xi,f(\tau))dB(\tau), \quad 0 < \gamma \leq 1, \tag{1.2}$$

subject to the initial condition:

$$f(0) = \delta_0, \tag{1.3}$$

where $f, g, \mathcal{K}_1$, and $\mathcal{K}_2$ are stochastic processes defined on the common probability space $(\Omega, \mathcal{F}, P)$, and f representing the unknown function. $B(t)$ represents the Brownian motion process and the second integral in Eq. (1.1) is an Itô integral. Also, D^{γ} denotes the Caputo fractional derivative of order $0 < \gamma \leq 1$ which is defined as [33]:

$$D^{\gamma}f(\xi) = \frac{1}{\Gamma(1-\gamma)} \int_0^{\xi} (\xi-\tau)^{-\gamma} f'(\tau)d\tau. \tag{1.4}$$

Proposition 1.1. *Let $f(s,\tau) = f(s)$ be a continuous function of bounded variation that depends only on a single variable. Then ([25, 43]):*

$$\int_0^{\xi} f(s)dB_s = f(\xi)B_{\xi} - \int_0^{\xi} B_s df_s. \tag{1.5}$$

2. Preliminary notes

2.1. **Fractional-order Genocchi wavelets.** The FGWs $\Psi_{n,m,\alpha}(t) = \Psi(k,n,m,\alpha,t)$ are specified over $[0,1)$ as:

$$\Psi_{n,m,\alpha}(t) = \begin{cases} 2^{\frac{k-1}{2}} \tilde{G}^*_m(2^{k-1}t - \hat{n}), & \frac{\hat{n}}{2^{k-1}} \leq t < \frac{\hat{n}+1}{2^{k-1}}, \\ 0, & \text{Otherwise}, \end{cases} \tag{2.1}$$

with

$$\tilde{G}^*_m(t) = \begin{cases} 1, & m = 1, \\ \frac{1}{\sqrt{\frac{2(-1)^m (m!)^2}{(2m)!\alpha}}} G^*_m(t), & m > 1, \end{cases} \tag{2.2}$$

where k is a integer number, $n = 1, 2, \ldots, 2^{k-1}$, indicates the number of subintervals, $m = 1, 2, \ldots, M$ is the degree of the Genocchi polynomial, $0 < \alpha \leq 1$, and $G^*_m(t)$ is the fractional-order Genocchi function which is provided within the interval $[0,1]$ as [8]

$$G^*_m(t) = \sum_{i=0}^{m} \binom{m}{i} g_{m-i} t^{i\alpha}, \tag{2.3}$$

where g_m denotes the m-th Bernoulli number.

2.2. **Introduction of activation functions.** In this section, we introduce a novel algorithm that utilizes two classes of activation functions (AF) to approximate solutions of the SFIDEs and IVIEs.

A general activation function for solving an equation can be expressed as:

$$\mathcal{N}(\xi, C) = AF(\Theta), \tag{2.4}$$

depending on a linear combination Θ of the basis functions, where in this instance, the basis functions are the FGWs:

$$\Theta = \sum_{n=1}^{2^{k-1}} \sum_{m=1}^{M} c_{n,m} \Psi^*_{n,m,\alpha}(\xi). \tag{2.5}$$

Here, the coefficient vector C and the wavelet vector $\Psi(t)$ are defined as:

$$C = [c_{1,1}, \ldots, c_{1,M}, c_{2,1}, \ldots, c_{2,M}, \ldots, c_{2^{k-1},M}]^T,$$
$$\Psi^*_{n,m,\alpha}(\xi) = [\Psi_{1,1,\alpha}(\xi), \ldots, \Psi_{1,M,\alpha}(\xi), \ldots, \Psi_{2^{k-1},1,\alpha}(\xi), \ldots, \Psi_{2^{k-1},M,\alpha}(\xi)]^T.$$

In this framework, the activation function operates on a linear combination of the FGWs. Specifically, we employ the inverse hyperbolic sine function, Arcsinh(ξ), as the activation function. Figures 1 and 2 display the graphs of $\psi_{n,m,\alpha}(\xi)$ and $Arcsinh(\psi_{n,m,\alpha}(\xi))$ for $k = 2, M = 4$ with $\alpha = 1$ and $\frac{1}{2}$, respectively.

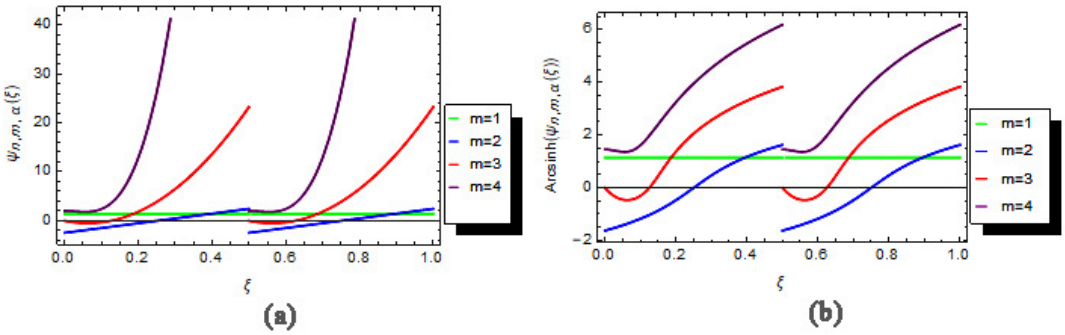

FIGURE 1. Plot of (a): $\psi_{n,m,\alpha}(\xi)$, (b): $Arcsinh(\psi_{n,m,\alpha}(\xi))$ for $\alpha = 1$.

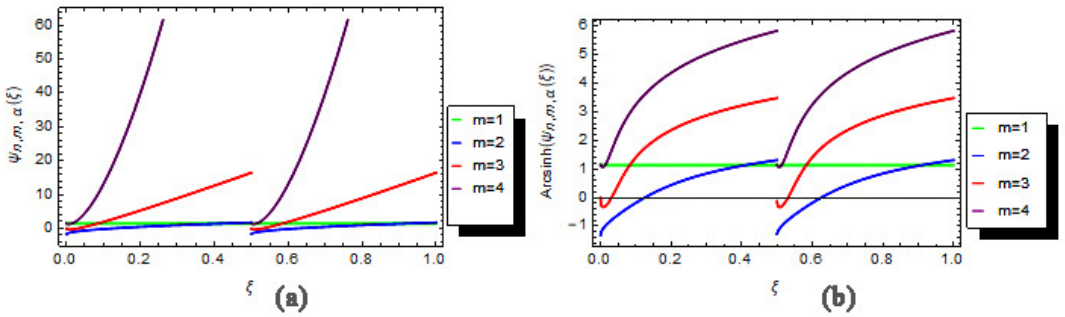

FIGURE 2. Plot of (a): $\psi_{n,m,\alpha}(\xi)$, (b): $Arcsinh(\psi_{n,m,\alpha}(\xi))$ for $\alpha = \frac{1}{2}$.

3. Numerical approach

The primary objective of this section is to introduce a numerical technique based on AFs and collocation method (AFsCM) to solve SFIDEs and IVIEs.

3.1. **Type 1.**

To solve Eq. (1.1), we approximate function f by means of an AF of the form

$$f(\xi) \simeq \tilde{f}(\xi) = \mathcal{N}(\xi, C). \tag{3.1}$$

We substitute Eq. (3.1) into Eq. (1.1) to obtain

$$\tilde{f}(\xi) = g(\xi) + \int_0^\xi \mathcal{K}_1(\tau, \xi, \tilde{f}(\tau))d\tau + \int_0^\xi \mathcal{K}_2(\tau, \xi, \tilde{f}(\tau))dB(\tau) + Res_{k,M}(\xi), \tag{3.2}$$

where $Res_{k,M}(\xi), \xi \in [0,1]$ is the residual error.

By using Proposition 1.1, we get

$$\tilde{f}(\xi) = g(\xi) + \int_0^{\xi} \mathcal{K}_1(\tau,\xi,\tilde{f}(\tau))d\tau + \mathcal{K}_2(\xi,\xi,\tilde{f}(\xi))B(\xi) - \int_0^{\xi} \mathcal{H}(\tau,\xi,\tilde{f}(\tau))B(\tau)d\tau + Res_{k,M}(\xi), \tag{3.3}$$

where

$$\mathcal{H}(\tau,\xi,f(\tau)) = \tfrac{\partial}{\partial\tau}\mathcal{K}_2(\tau,\xi,f(\tau)).$$

For computing the integral parts of Eq. (3.3), we employ the GLQR [42]. Then, we achieve

$$\begin{aligned}\tilde{f}(\xi) = g(\xi) &+ \frac{\xi}{2}\sum_{j=1}^{\tilde{n}} \omega_j \mathcal{K}_1\Big(\frac{\xi}{2}\eta_j + \frac{\xi}{2}, \xi, \tilde{f}(\frac{\xi}{2}\eta_j + \frac{\xi}{2})\Big) + \mathcal{K}_2(\xi,\xi,\tilde{f}(\xi))B(\xi)\\ &- \frac{\xi}{2}\sum_{j=1}^{\hat{n}} \omega_j \mathcal{H}\Big(\frac{\xi}{2}\eta_j + \frac{\xi}{2}, \xi, \tilde{f}(\frac{\xi}{2}\eta_j + \frac{\xi}{2})\Big)B(\frac{\xi}{2}\eta_j + \frac{\xi}{2}) + Res_{k,M}(\xi),\end{aligned} \tag{3.4}$$

where $Res_{k,M}(\xi)$ is the residual error function.

Now, by collocating Eq. (3.4) at zeros of the shifted Legendre polynomial ($L_{2^{k-1}M}(\xi)$), we have

$$\begin{aligned}\tilde{f}(\xi_i) \simeq g(\xi_i) &+ \frac{\xi_i}{2}\sum_{j=1}^{\tilde{n}} \omega_j \mathcal{K}_1\Big(\frac{\xi_i}{2}\eta_j + \frac{\xi_i}{2}, \xi_i, \tilde{f}(\frac{\xi_i}{2}\eta_j + \frac{\xi_i}{2})\Big) + \mathcal{K}_2(\xi_i,\xi_i,\tilde{f}(\xi_i))B(\xi_i)\\ &- \frac{\xi_i}{2}\sum_{j=1}^{\hat{n}} \omega_j \mathcal{H}\Big(\frac{\xi_i}{2}\eta_j + \frac{\xi_i}{2}, \xi_i, \tilde{f}(\frac{\xi_i}{2}\eta_j + \frac{\xi_i}{2})\Big)B(\frac{\xi_i}{2}\eta_j + \frac{\xi_i}{2}).\end{aligned} \tag{3.5}$$

By considering $i = 1, \ldots, 2^{k-1}M$ in Eq. (3.5), we achieve a system of algebraic equations with $2^{k-1}M$ equations and $2^{k-1}M$ unknown coefficients. This system can be addressed by employing Newton's iterative approach to approximate the solution of f.

Remark 3.1. For the smooth function, f, the GLQR is defined as ([31, 42]):

$$\int_a^b f(\xi)d\xi \simeq \tfrac{b-a}{2}\sum_{r=1}^{n^\star} \omega_r f(a + (\eta_r + 1)\tfrac{b-a}{2}),$$

where $\eta_r, r = 1, 2, \ldots n^\star$, are zeros of the Legendre polynomial $L_{n^\star}(\zeta)$ and $\omega_r = \frac{-2}{(n^\star+1)L'_{n^\star}(\eta_r)L_{n^\star+1}(\eta_r)}, r = 1, 2, \ldots, n^\star$.

3.2. **Type 2.** According to the definition of the Caputo fractional derivative in Eq. (1.4), the numerical method for solving FDEs necessitates the values of the solution at preceding time steps. Consequently, a significant amount of memory is required to store the data during computation, which might exceed the available memory capacity of the computing device. Hence, initially, we approximate the Caputo fractional derivative ($0 < \gamma \leq 1$) by employing the Laplace transform technique, akin to the approach outlined in [37], as follows:

$$L\{D^\gamma f(\xi)\} = s^\gamma \hat{f}(s) - s^{\gamma-1}f(0), \tag{3.6}$$

where $\hat{f}(s)$ represents the Laplace transform of $f(\xi)$. We approximate the term s^γ linearly as

$$s^\gamma \simeq \gamma s^1 + (1-\gamma)s^0 = \gamma s + (1-\gamma). \tag{3.7}$$

Substituting Eq. (3.7) into Eq. (3.6), we derive

$$L\{D^\gamma f(\xi)\} \simeq \gamma s[\hat{f}(s) - s^{-1}f(0)] + (1-\gamma)[\hat{f}(s) - s^{-1}f(0)]. \tag{3.8}$$

Applying the inverse Laplace transform, yields

$$D^\gamma f(\xi) \simeq \gamma f'(\xi) + (1-\gamma)(f(\xi) - f(0)). \tag{3.9}$$

By substituting Eq. (3.9) in Eq. (1.2), we achieve

$$\gamma f'(\xi) + (1-\gamma)(f(\xi) - \delta_0) = g(\xi) + \int_0^{\xi} \mathcal{K}_1(\tau,\xi,f(\tau))d\tau + \int_0^{\xi} \mathcal{K}_2(\tau,\xi,f(\tau))dB(\tau), \tag{3.10}$$

where δ_0 is the initial condition.

Now, we solve Eq. (3.10) instead of Eq. (1.2). To get the approximate solution of Eq. (3.10), we approximate function f using an AF in the form

$$f(\xi) \simeq \tilde{f}(\xi) = \delta_0 + \xi \mathcal{N}(\xi, C). \tag{3.11}$$

We substitute Eq. (3.11) into Eq. (3.10), then it yields

$$\gamma \tilde{f}'(\xi) + (1-\gamma)(\tilde{f}(\xi) - \delta_0) = g(\xi) + \int_0^\xi \mathcal{K}_1(\tau, \xi, \tilde{f}(\tau))d\tau + \int_0^\xi \mathcal{K}_2(\tau, \xi, \tilde{f}(\tau))dB(\tau). \tag{3.12}$$

By using Eqs. (3.10)-(3.12), the GLQR, Proposition 1.1, and collocation approach, we have

$$\begin{aligned}\gamma \tilde{f}'(\xi) + (1-\gamma)(\tilde{f}(\xi) - \delta_0) = g(\xi) &+ \frac{\xi}{2}\sum_{j=1}^{\tilde{n}} \omega_j \mathcal{K}_1\Big(\frac{\xi}{2}\eta_j + \frac{\xi}{2}, \xi, \tilde{f}(\frac{\xi}{2}\eta_j + \frac{\xi}{2})\Big) + \mathcal{K}_2(\xi, \xi, \tilde{f}(\xi))B(\xi) \\ &- \frac{\xi}{2}\sum_{j=1}^{\tilde{n}} \omega_j \mathcal{H}\Big(\frac{\xi}{2}\eta_j + \frac{\xi}{2}, \xi, \tilde{f}(\frac{\xi}{2}\eta_j + \frac{\xi}{2})\Big)B(\frac{\xi}{2}\eta_j + \frac{\xi}{2}).\end{aligned} \tag{3.13}$$

Collocating Eq. (3.13) at zeros of the shifted Legendre polynomial ($L_{2^{k-1}M}(\xi)$), we get

$$\begin{aligned}&\gamma \tilde{f}'(\xi_i) + (1-\gamma)(\tilde{f}(\xi_i) - \delta_0) - g(\xi_i) - \frac{\xi_i}{2}\sum_{j=1}^{\tilde{n}} \omega_j \mathcal{K}_1\Big(\frac{\xi_i}{2}\eta_j + \frac{\xi_i}{2}, \xi_i, \tilde{f}(\frac{\xi_i}{2}\eta_j + \frac{\xi_i}{2})\Big) \\ &- \mathcal{K}_2(\xi_i, \xi_i, \tilde{f}(\xi_i))B(\xi_i) + \frac{\xi_i}{2}\sum_{j=1}^{\tilde{n}} \omega_j \mathcal{H}\Big(\frac{\xi_i}{2}\eta_j + \frac{\xi_i}{2}, \xi_i, \tilde{f}(\frac{\xi_i}{2}\eta_j + \frac{\xi_i}{2})\Big)B(\frac{\xi_i}{2}\eta_j + \frac{\xi_i}{2}) = 0.\end{aligned} \tag{3.14}$$

Eq. (3.14) denotes a system of $2^{k-1}M$ equations with $2^{k-1}M$ unknown coefficients that can be solved via Newton's iterative approach. In fact, we use "Find Root" package at Mathematica software.

4. Convergence analysis

The aim of this part is to demonstrate the convergence of the mentioned numerical method for SEs of Type 1. In this section, the norm is defined by

$$\|f\|^2 = E[|f|^2]. \tag{4.1}$$

Theorem 4.1. *Assume that $f(\xi)$ and $\tilde{f}(\xi)$ represent the exact and numerical solutions, respectively, of the problem (1.1). Additionally, suppose that*
(i) functions $\mathcal{K}_1(x,t,f(x)), \mathcal{K}_2(x,t,f(x))$ and $\mathcal{H}(x,t,f(x))$ satisfy the Lipschitz condition, i.e.,

$$\begin{aligned}|\mathcal{K}_1(x,t,f(x)) - \mathcal{K}_1(x,t,\tilde{f}(x))| &\le \theta_1|f(x) - \tilde{f}(x)|, \\ |\mathcal{K}_2(x,t,f(x)) - \mathcal{K}_2(x,t,\tilde{f}(x))| &\le \theta_2|f(x) - \tilde{f}(x)|, \\ |\mathcal{H}(x,t,f(x)) - \mathcal{H}(x,t,\tilde{f}(x))| &\le \theta|f(x) - \tilde{f}(x)|,\end{aligned}$$

where $x, t \in [0,1)$ and $f, \tilde{f}$ belong to the probability space $(\Omega, \mathcal{F}, P)$.
(ii) $1 - 8\theta_1^2 - 4\theta_2^2 - 8\theta^2 > 0$,
then we have

$$\|\mathcal{E}\|^2 = \|f - \tilde{f}\|^2 \le \frac{8\|E_{1,\tilde{n}}\|^2 + 8\|E_{2,\hat{n}}\|^2 + 4\|Res_{k,M}\|^2}{1 - 8\theta_1^2 - 4\theta_2^2 - 8\theta^2}, \tag{4.2}$$

where $\|E_{1,\tilde{n}}\|$ and $\|E_{2,\hat{n}}\|$ are the errors of the GLQR, when applied to the first and second integrals of Equation (3.3), respectively.

Proof. From Eqs. (1.1) and (3.4), we have

$$f(\xi) = g(\xi) + \int_0^\xi \mathcal{K}_1(\tau,\xi,f(\tau))d\tau + \mathcal{K}_2(\xi,\xi,f(\xi))B(\xi) - \int_0^\xi \mathcal{H}(\tau,\xi,f(\tau))B(\tau)d\tau, \tag{4.3}$$

and

$$\begin{aligned}\tilde{f}(\xi) = g(\xi) &+ \frac{\xi}{2}\sum_{j=1}^{\tilde{n}} \omega_j \mathcal{K}_1\Big(\frac{\xi}{2}\eta_j + \frac{\xi}{2}, \xi, \tilde{f}(\frac{\xi}{2}\eta_j + \frac{\xi}{2})\Big) + \mathcal{K}_2(\xi,\xi,\tilde{f}(\xi))B(\xi)\\ &- \frac{\xi}{2}\sum_{j=1}^{\hat{n}} \omega_j \mathcal{H}\Big(\frac{\xi}{2}\eta_j + \frac{\xi}{2}, \xi, \tilde{f}(\frac{\xi}{2}\eta_j + \frac{\xi}{2})\Big)B(\frac{\xi}{2}\eta_j + \frac{\xi}{2}) + Res_{k,M}(\xi).\end{aligned} \tag{4.4}$$

Subtracting Eq. (4.4) from Eq. (4.3), we obtain

$$\begin{aligned}f(\xi) - \tilde{f}(\xi) &= \int_0^\xi \mathcal{K}_1(\tau,\xi,f(\tau))d\tau - \frac{\xi}{2}\sum_{j=1}^{\tilde{n}} \omega_j \mathcal{K}_1\Big(\frac{\xi}{2}\eta_j + \frac{\xi}{2}, \xi, \tilde{f}(\frac{\xi}{2}\eta_j + \frac{\xi}{2})\Big)\\ &+ \mathcal{K}_2(\xi,\xi,f(\xi))B(\xi) - \mathcal{K}_2(\xi,\xi,\tilde{f}(\xi))B(\xi) - \int_0^\xi \mathcal{H}(\tau,\xi,f(\tau))B(\tau)d\tau\\ &+ \frac{\xi}{2}\sum_{j=1}^{\hat{n}} \omega_j \mathcal{H}\Big(\frac{\xi}{2}\eta_j + \frac{\xi}{2}, \xi, \tilde{f}(\frac{\xi}{2}\eta_j + \frac{\xi}{2})\Big)B(\frac{\xi}{2}\eta_j + \frac{\xi}{2}) - Res_{k,M}(\xi)\\ &= \mathcal{L}_1(\xi) + \mathcal{L}_2(\xi) + \mathcal{L}_3(\xi) + \mathcal{L}_4(\xi).\end{aligned} \tag{4.5}$$

We have

$$\mathcal{L}_1(\xi) = \int_0^\xi \mathcal{K}_1(\tau,\xi,f(\tau))d\tau - \frac{\xi}{2}\sum_{j=1}^{\tilde{n}} \omega_j \mathcal{K}_1\Big(\frac{\xi}{2}\eta_j + \frac{\xi}{2}, \xi, \tilde{f}(\frac{\xi}{2}\eta_j + \frac{\xi}{2})\Big). \tag{4.6}$$

From Eq. (4.6), and the error of the GLQR, we achieve

$$\begin{aligned}|\mathcal{L}_1(\xi)| &\le \Big|\int_0^\xi \mathcal{K}_1(\tau,\xi,f(\tau))d\tau - \frac{\xi}{2}\sum_{j=1}^{\tilde{n}} \omega_j \mathcal{K}_1\Big(\frac{\xi}{2}\eta_j + \frac{\xi}{2}, \xi, \tilde{f}(\frac{\xi}{2}\eta_j + \frac{\xi}{2})\Big)\Big|\\ &\le \Big|\int_0^\xi \mathcal{K}_1(\tau,\xi,f(\tau))d\tau - \int_0^\xi \mathcal{K}_1(\tau,\xi,\tilde{f}(\tau))d\tau\Big|\\ &+ \Big|\int_0^\xi \mathcal{K}_1(\tau,\xi,\tilde{f}(\tau))d\tau - \frac{\xi}{2}\sum_{j=1}^{\tilde{n}} \omega_j \mathcal{K}_1\Big(\frac{\xi}{2}\eta_j + \frac{\xi}{2}, \xi, \tilde{f}(\frac{\xi}{2}\eta_j + \frac{\xi}{2})\Big)\Big|\\ &\le \int_0^\xi |\mathcal{K}_1(\tau,\xi,f(\tau)) - \mathcal{K}_1(\tau,\xi,\tilde{f}(\tau))|d\tau\\ &+ \Big|\int_0^\xi \mathcal{K}_1(\tau,\xi,\tilde{f}(\tau))d\tau - \frac{\xi}{2}\sum_{j=1}^{\tilde{n}} \omega_j \mathcal{K}_1\Big(\frac{\xi}{2}\eta_j + \frac{\xi}{2}, \xi, \tilde{f}(\frac{\xi}{2}\eta_j + \frac{\xi}{2})\Big)\Big|\\ &\le \theta_1 \int_0^\xi |f(\tau) - \tilde{f}(\tau)|d\tau + |E_{1,\tilde{n}}|.\end{aligned} \tag{4.7}$$

So, we have

$$|\mathcal{L}_1(\xi)| \le \theta_1 \int_0^\xi |f(\tau) - \tilde{f}(\tau)|d\tau + |E_{1,\tilde{n}}|. \tag{4.8}$$

Using $(a+b)^2 \leq 2a^2+2b^2$, for $\mathcal{L}_1(\xi)$, we yield

$$|\mathcal{L}_1(\xi)|^2 \leq 2\theta_1^2(\int_0^\xi |f(\tau)-\tilde{f}(\tau)|d\tau)^2 + 2|E_{1,\tilde{n}}|^2. \tag{4.9}$$

From the Schwarz inequality, and $0 \leq \xi \leq 1$, we have

$$|\mathcal{L}_1(\xi)|^2 \leq 2\theta_1^2 \int_0^1 |f(\tau)-\tilde{f}(\tau)|^2 d\tau + 2|E_{1,\tilde{n}}|^2. \tag{4.10}$$

Taking expectations implies

$$\|\mathcal{L}_1\|^2 \leq 2\theta_1^2\|f-\tilde{f}\|^2 + 2\|E_{1,\tilde{n}}\|^2. \tag{4.11}$$

Remark 4.2. By using $B(t) \sim \sqrt{t}N(0,1)$ and definition of norm, we get

$$\|B(t)\|^2 = E(B(t)^2) = t,$$

so, $\|B(t)\| \leq 1$ for $t \in [0,1)$.

For $\mathcal{L}_2(\xi)$, we get

$$|\mathcal{L}_2(\xi)| = |\mathcal{K}_2(\xi,\xi,f(\xi))B(\xi) - \mathcal{K}_2(\xi,\xi,\tilde{f}(\xi))B(\xi)| \leq \theta_2|B(\xi)||\mathcal{E}(\xi)| \leq \theta_2|\mathcal{E}(\xi)|. \tag{4.12}$$

So

$$|\mathcal{L}_2(\xi)|^2 \leq \theta_2^2|\mathcal{E}(\xi)|^2. \tag{4.13}$$

Taking expectations from Eq. (4.13), we have

$$\|\mathcal{L}_2\|^2 \leq \theta_2^2\|\mathcal{E}\|^2. \tag{4.14}$$

For $\mathcal{L}_3(\xi)$, we obtain

$$\mathcal{L}_3(\xi) = \int_0^\xi \mathcal{H}(\tau,\xi,f(\tau))B(\tau)d\tau - \frac{\xi}{2}\sum_{j=1}^{\hat{n}} \omega_j \mathcal{H}\Big(\frac{\xi}{2}\eta_j + \frac{\xi}{2}, \xi, \tilde{f}(\frac{\xi}{2}\eta_j + \frac{\xi}{2})\Big) B(\frac{\xi}{2}\eta_j + \frac{\xi}{2}). \tag{4.15}$$

Using Eq. (4.15), and the error of the GLQR, we obtain

$$\begin{aligned}
|\mathcal{L}_3(\xi)| &\leq \Big| \int_0^\xi \mathcal{H}(\tau,\xi,f(\tau))B(\tau)d\tau - \frac{\xi}{2}\sum_{j=1}^{\hat{n}} \omega_j \mathcal{H}\Big(\frac{\xi}{2}\eta_j + \frac{\xi}{2}, \xi, \tilde{f}(\frac{\xi}{2}\eta_j + \frac{\xi}{2})\Big) B(\frac{\xi}{2}\eta_j + \frac{\xi}{2}) \Big| \\
&\leq \Big| \int_0^\xi \mathcal{H}(\tau,\xi,f(\tau))B(\tau)d\tau - \int_0^\xi \mathcal{H}(\tau,\xi,\tilde{f}(\tau))B(\tau)d\tau \Big| \\
&+ \Big| \int_0^\xi \mathcal{H}(\tau,\xi,\tilde{f}(\tau))B(\tau)d\tau - \frac{\xi}{2}\sum_{j=1}^{\hat{n}} \omega_j \mathcal{H}\Big(\frac{\xi}{2}\eta_j + \frac{\xi}{2}, \xi, \tilde{f}(\frac{\xi}{2}\eta_j + \frac{\xi}{2})\Big) B(\frac{\xi}{2}\eta_j + \frac{\xi}{2}) \Big| \\
&\leq \int_0^\xi |\mathcal{H}(\tau,\xi,f(\tau))B(\tau) - \mathcal{H}(\tau,\xi,\tilde{f}(\tau))B(\tau)|d\tau \\
&+ \Big| \int_0^\xi \mathcal{H}(\tau,\xi,\tilde{f}(\tau))B(\tau)d\tau - \frac{\xi}{2}\sum_{j=1}^{\hat{n}} \omega_j \mathcal{H}\Big(\frac{\xi}{2}\eta_j + \frac{\xi}{2}, \xi, \tilde{f}(\frac{\xi}{2}\eta_j + \frac{\xi}{2})\Big) B(\frac{\xi}{2}\eta_j + \frac{\xi}{2}) \Big| \\
&\leq \theta \int_0^\xi |B(\tau)||f(\tau)-\tilde{f}(\tau)|d\xi + |E_{2,\hat{n}}|.
\end{aligned} \tag{4.16}$$

So, we get

$$|\mathcal{L}_3(\xi)| \leq \theta \int_0^{\xi} |B(\tau)||f(\tau) - \tilde{f}(\tau)|d\xi + |E_{2,\hat{n}}|. \tag{4.17}$$

Using $(a+b)^2 \leq 2a^2 + 2b^2$, for $\mathcal{L}_1(\xi)$, we achieve

$$|\mathcal{L}_3(\xi)|^2 \leq 2\theta^2 (\int_0^{\xi} |B(\tau)||f(\tau) - \tilde{f}(\tau)|d\xi)^2 + 2|E_{2,\hat{n}}|^2. \tag{4.18}$$

From Schwarz inequality, and $0 \leq \xi \leq 1$, we have

$$|\mathcal{L}_3(\xi)|^2 \leq 2\theta^2 \int_0^{1} |f(\tau) - \tilde{f}(\tau)|^2 d\xi + 2|E_{2,\hat{n}}|^2. \tag{4.19}$$

Taking expectations implies

$$\|\mathcal{L}_3\|^2 \leq 2\theta^2 \|\mathcal{E}\|^2 + 2\|E_{2,\hat{n}}\|^2. \tag{4.20}$$

$$\|\mathcal{L}_4\|^2 = \|Res_{k,M}\|^2. \tag{4.21}$$

By applying $(a+b+c+d)^2 \leq 4a^2 + 4b^2 + 4c^2 + 4d^2$, we get

$$\|\mathcal{E}\|^2 \leq 4\|\mathcal{L}_1\|^2 + 4\|\mathcal{L}_2\|^2 + 4\|\mathcal{L}_3\|^2 + 4\|\mathcal{L}_4\|^2. \tag{4.22}$$

From Eqs. (4.11), (4.14), (4.20), and (4.22), we have

$$\|\mathcal{E}\|^2 \leq \frac{8\|E_{1,\tilde{n}}\|^2 + 8\|E_{2,\hat{n}}\|^2 + 4\|Res_{k,M}\|^2}{1 - 8\theta_1^2 - 4\theta_2^2 - 8\theta^2}. \tag{4.23}$$

This completes the proof. □

We report the values of $\|\mathcal{E}\|$ for Example 5.1, in Table 2.

Remark 4.3. Theorem 4.1 establishes an a posteriori estimate for the absolute error $\|\mathcal{E}\|$, in terms of the norms of the residual error $\|Res_{k,M}\|$ and the error of the Gaussian quatratures. That is, we have shown that if $\|Res_{k,M}\|$, $\|E_{1,\tilde{n}}\|$, and $\|E_{2,\hat{n}}\|$ tend to zero (as $\tilde{n}, \hat{n}, k$ and M tend to ∞) then the method is convergent (provided that θ_1, θ_2, and θ are sufficiently small). The convergence of $\|E_{1,\tilde{n}}\|$ and $\|E_{2,\hat{n}}\|$ is well established from classical results of numerical analysis, under the condition that f is sufficiently smooth. Concerning $\|Res_{k,M}\|$, it can be evaluated numerically in each case. The numerical examples in section 5 (see Tables 2 and 12) provide numerical evidence that for a regular function $\|Res_{k,M}\|$ converges fast to 0 as M tends to infinity. The conditions under which $\|Res_{k,M}\|$ converges to 0 are so far an open question and will be subject of further research.

5. Illustrative test problems

In the current part, we have carried out the proposed approach to compute the numerical solution of some SFIDEs and IVIEs to illustrate the accuracy and efficiency of our scheme. The computations associated with the examples were performed using Mathematica 10 on a computer with a 2.67 GHz Intel Core i5 processor and 4 GB of RAM.

5.1. **Type 1.**

Example 5.1. Let's examine the linear IVIE given by [13]

$$f(\xi) = 1 + \int_0^{\xi} \tau^2 f(\tau)d\tau + \int_0^{\xi} \tau f(\tau)dB(\tau), \quad 0 \leq \tau, \xi \leq 0.5. \tag{5.1}$$

The exact solution of the aforementioned problem is

$$f(\xi) = exp\left(\frac{t^3}{6} + \int_0^{t} \tau dB(\tau)\right). \tag{5.2}$$

Table 1 reports the exact and numerical results of the generalized hat functions approach with $n = 32, m = 25$ and the suggested scheme with $k = 2, M = 10$. This table shows that using only a small number of FGWs improves the

accuracy of the results. The residual errors and the CPU time for $k = 2, \alpha = 1$ and several cases M are demonstrated in Table 2. This table confirms that increasing the degree M of the FGWs, the results become more accurate.

TABLE 1. The exact and numerical results with $\alpha = 1$ (Example 5.1).

ξ	*Hat functions method* $n = 32, m = 25$		*Proposed strategy* $k = 2, M = 10$	
	Exact	*Numerical*	*Exact*	*Numerical*
0.1	0.9669176	0.9684280	1.0059190	1.0060866
0.2	1.0105371	1.0066520	1.0246190	1.0259860
0.3	1.0378587	1.0460315	1.0580224	1.0627942
0.4	1.0760953	1.0823571	1.1089153	1.1208071
0.5	0.9907228	1.0118890	1.1812772	1.2060363

TABLE 2. The residual errors with $k = 2, \alpha = 1$ for diverse quantities of M (Example 5.1).

ξ	$M = 4$	$M = 6$	$M = 8$	$M = 10$
0.1	6.93×10^{-7}	1.86×10^{-7}	4.47×10^{-8}	5.25×10^{-11}
0.2	1.94×10^{-5}	1.57×10^{-7}	6.02×10^{-8}	2.01×10^{-10}
0.3	6.11×10^{-5}	1.10×10^{-6}	6.93×10^{-7}	9.69×10^{-10}
0.4	2.81×10^{-5}	1.01×10^{-5}	6.03×10^{-6}	1.25×10^{-8}
$\|\mathcal{E}\|$	1.59×10^{-4}	2.15×10^{-5}	2.47×10^{-7}	4.49×10^{-8}
CPU	0.265	0.937	2.859	4.141

Example 5.2. Let's examine the linear IVIE given by [13]

$$f(\xi) = \frac{1}{12} + \int_0^{\xi} \cos(\tau) f(\tau) d\tau + \int_0^{\xi} \sin(\tau) f(\tau) dB(\tau), \quad 0 \le \tau, \xi \le 0.5. \tag{5.3}$$

The exact solution of the aforementioned problem is

$$f(\xi) = \frac{1}{12} exp\Big(-\frac{t}{4} + \sin(t) + \frac{\sin(2t)}{8} + \int_0^t \sin(\tau) dB(\tau) \Big). \tag{5.4}$$

Table 3 compares the exact solution with numerical results obtained using with $n = 32, m = 25$ and the suggested scheme with $k = 2, M = 10$. Figure 3 displays the residual errors for $M = 10$, and $\alpha = 0.25$ with $k = 1, 2$.

TABLE 3. The exact and numerical results with $\alpha = \frac{1}{4}$ (Example 5.2).

ξ	*Hat functions method* $n = 32, m = 25$		*Proposed strategy* $k = 2, M = 10$	
	Exact	*Numerical*	*Exact*	*Numerical*
0.1	0.0890088	0.0891427	0.0921674	0.0921835
0.2	0.1024286	0.1020402	0.1019567	0.1020924
0.3	0.1151393	0.1160338	0.1125844	0.1130838
0.4	0.1294754	0.1301881	0.1238629	0.1251497
0.5	0.1283848	0.1309717	0.1355298	0.1429448

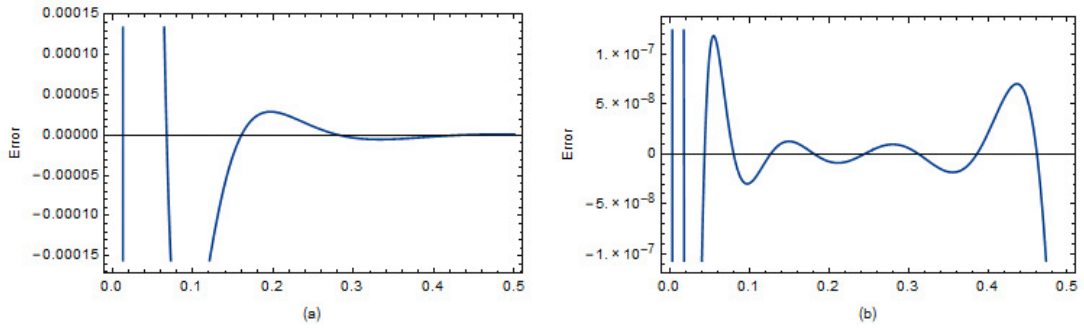

FIGURE 3. The residual errors for $M = 10$ and $\alpha = 0.25$ with (a): $k = 1$, (b): $k = 2$. (Example 5.2).

Example 5.3. Let's examine the following nonlinear IVIE studied in [22]

$$f(\xi) = 0.5 + \int_0^{\xi} f(\tau)(1 - f(\tau))d\tau + 0.25 \int_0^{\xi} f(\tau)dB(\tau), \quad 0 \leq \tau, \xi \leq 1. \tag{5.5}$$

The exact solution of the aforementioned problem is

$$f(\xi) = \frac{0.5exp(0.96875\xi + 0.25B(\xi))}{1 + 0.5\int_0^{\xi} exp(0.96875\tau + 0.25B(\tau))d\tau}. \tag{5.6}$$

In Table 4, we present a comparison of the absolute error for the discussed approach for $k = 1, M = 4, \alpha = \frac{1}{4}$ with the block-pulse method and the Euler method for $N = 4$. Also, Figure 4 shows the numerical and exact solutions with $k = 1, M = 4$ for $\alpha = 1, \frac{1}{4}$.

TABLE 4. The absolute error with $k = 1, \alpha = \frac{1}{4}$ (Example 5.3).

ξ	*Block − pulse method* $N = 4$	*Euler method* $N = 4$	*Proposed strategy* $M = 4$
0.1	0.0085	0.0267	0.0009
0.2	0.0100	0.0450	0.0025
0.3	0.1072	0.0309	0.0049
0.4	0.1256	0.0267	0.0071
0.5	0.1168	0.0062	0.0090
0.6	0.2080	0.0600	0.0106
0.7	0.2430	0.0694	0.0122
0.8	0.2832	0.0843	0.0138
0.9	0.3165	0.0933	0.0156
CPU	–	–	0.109

Example 5.4. Let's examine the nonlinear IVIE given by [22]

$$f(\xi) = 1 + \int_0^{\xi} f(\tau)(\frac{1}{32} - f^2(\tau))d\tau + 0.25 \int_0^{\xi} f(\tau)dB(\tau), \quad 0 \leq \tau, \xi \leq 1. \tag{5.7}$$

The exact solution of this problem is

$$f(\xi) = \frac{exp(0.25B(\xi))}{\sqrt{1 + 2\int_0^{\xi} exp(0.5B(\tau))d\tau}}. \tag{5.8}$$

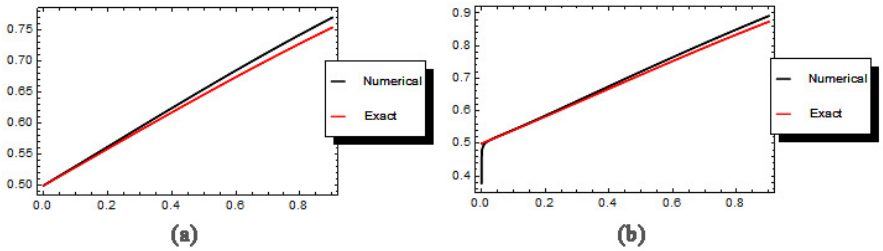

FIGURE 4. The graphs of the numerical and exact solution with $k = 1, M = 4$ for $(a) : \alpha = 1, (b) : \alpha = \frac{1}{4}$ (Example 5.3).

In Table 5, we compare the absolute error of the mentioned scheme for $k = 1, M = 4, \alpha = \frac{3}{4}$ with the block-pulse method and the Euler method for $N = 4$. Also,Figure 5 shows the numerical and exact solutions with $k = 1, M = 4$ for $\alpha = 1, \frac{3}{4}$. This figure demonstrates the influence of the fractional order parameter α.

TABLE 5. The absolute error with $k = 1, \alpha = \frac{3}{4}$ (Example 5.4).

ξ	*Block − pulse method* $N = 4$	*Euler method* $N = 4$	*Presented method* $M = 4$
0.1	0.0614	0.0529	0.0013
0.2	0.1198	0.0289	0.0037
0.3	0.1657	0.0067	0.0061
0.4	0.2024	0.0159	0.0079
0.5	0.2320	0.0412	0.0091
0.6	0.2560	0.0725	0.0099
0.7	0.2753	0.1141	0.0107
0.8	0.2903	0.1714	0.0114
0.9	0.3016	0.2512	0.0123
CPU	–	–	0.094

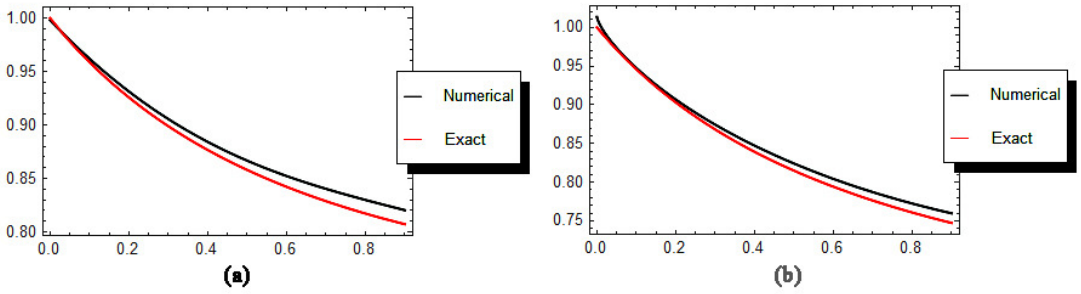

FIGURE 5. The plots of the numerical and exact solution with $k = 1, M = 4$ for $(a) : \alpha = 1, (b) : \alpha = \frac{3}{4}$ (Example 5.4).

5.2. **Type 2.**

Example 5.5. Let's examine the SFIDE given by [43]

$$\begin{cases} D^{\gamma} f(\xi) = \frac{\Gamma(2)\xi^{1-\gamma}}{\Gamma(2-\gamma)} - \frac{\xi^3}{3} + \int_0^{\xi} \tau f(\tau) d\tau + \int_0^{\xi} f(\tau) dB(\tau), \quad 0 \le \tau, \xi \le 1, \\ f(0) = 0. \end{cases} \tag{5.9}$$

We compare the residual errors of the mentioned algorithm for $k = 2, M = 10, \alpha = \frac{1}{2}$ with the shifted Legendre polynomial method with $N = 10$ in Table 6. Additionally, the CPU time is included in this table. Also, we report the residual errors and the CPU time via our approach for $k = 2, \gamma = 0.5$ and diverse values of α in Table 7. Table 7 demonstrates the influence of the parameter α. Figure 6 displays the numerical solutions for various values of γ with $k = 2, M = 10, \alpha = \frac{1}{2}$.

TABLE 6. The residual errors with $k = 2, \alpha = \frac{1}{2}$ (Example 5.5).

ξ	*Legendre polynomials method* $N = 10$			*Present method* $M = 10$		
	$\gamma = 0.25$	$\gamma = 0.5$	$\gamma = 0.75$	$\gamma = 0.25$	$\gamma = 0.5$	$\gamma = 0.75$
0.2	6.17×10^{-3}	7.93×10^{-3}	1.03×10^{-2}	5.87×10^{-8}	1.26×10^{-9}	5.00×10^{-7}
0.4	1.06×10^{-2}	1.12×10^{-2}	1.30×10^{-2}	3.39×10^{-7}	7.72×10^{-9}	2.13×10^{-6}
0.6	1.25×10^{-2}	1.28×10^{-2}	1.32×10^{-2}	2.52×10^{-5}	5.57×10^{-8}	1.37×10^{-7}
0.8	1.31×10^{-3}	1.64×10^{-3}	1.99×10^{-3}	9.64×10^{-5}	3.45×10^{-7}	6.46×10^{-6}
CPU	–	–	–	4.625	3.718	4.125

TABLE 7. The residual errors with $k = 2, \gamma = 0.5$ for various values of α (Example 5.5).

ξ	$\alpha = \frac{1}{4}$	$\alpha = \frac{1}{3}$	$\alpha = \frac{1}{2}$	$\alpha = \frac{3}{4}$	$\alpha = 1$
0.2	6.89×10^{-9}	5.28×10^{-8}	1.26×10^{-9}	2.08×10^{-5}	1.17×10^{-3}
0.4	2.76×10^{-8}	2.05×10^{-7}	7.72×10^{-9}	2.04×10^{-4}	2.94×10^{-2}
0.6	4.96×10^{-6}	1.62×10^{-5}	5.57×10^{-8}	2.68×10^{-4}	8.52×10^{-4}
0.8	1.40×10^{-6}	1.84×10^{-5}	3.45×10^{-7}	1.60×10^{-3}	2.64×10^{-2}
CPU	6.047	5.797	3.718	5.891	5.484

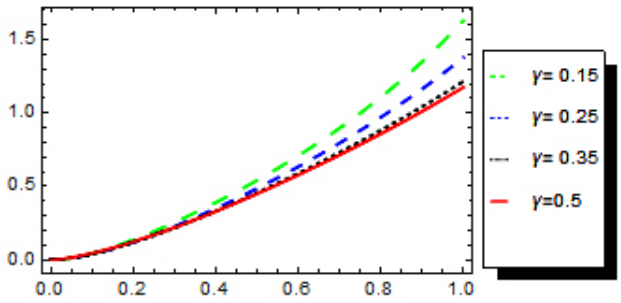

FIGURE 6. Approximate solutions with $k = 2, M = 10, \alpha = \frac{1}{2}$ for various values of γ (Example 5.5).

Example 5.6. Let's examine the SFIDE given by [43]

$$\begin{cases} D^{\gamma}f(\xi) = \frac{7\xi^4}{12} - \frac{5\xi^3}{6} + \frac{2\xi^{2-\gamma}}{\Gamma(3-\gamma)} + \frac{\xi^{1-\gamma}}{\Gamma(2-\gamma)} + \int_0^{\xi}(\tau+\xi)f(\tau)d\tau + \int_0^{\xi}\tau f(\tau)dB(\tau), \quad 0 \le \tau, \xi \le 1, \\ f(0) = 0. \end{cases} \tag{5.10}$$

The residual errors of the mentioned algorithm for $k = 2, M = 11, \alpha = \frac{1}{2}$ are compared with the shifted Legendre polynomial method for $N = 15$ in Table 8. Also, we present the residual errors and CPU time via the current scheme for $k = 2, \gamma = 0.5$ and diverse values of α in Table 9. Table 10 presents the numerical solutions for $k = 2, M = 11, \alpha = \frac{1}{2}$, and $\gamma = 0.25, 0.5, 0.75$. Figure 7 shows the numerical solutions and residual errors for different choices of γ with $k = 2, M = 10, \alpha = \frac{1}{2}$.

TABLE 8. The residual errors with $k = 2, \alpha = \frac{1}{2}$ (Example 5.6).

ξ	*Legendre polynomials method* $N = 15$			*Present method* $M = 11$		
	$\gamma = 0.25$	$\gamma = 0.5$	$\gamma = 0.75$	$\gamma = 0.25$	$\gamma = 0.5$	$\gamma = 0.75$
0.1	4.21×10^{-4}	5.28×10^{-4}	6.28×10^{-4}	3.14×10^{-8}	1.48×10^{-10}	3.88×10^{-7}
0.3	1.82×10^{-3}	1.88×10^{-3}	1.94×10^{-3}	9.35×10^{-8}	8.42×10^{-9}	9.10×10^{-7}
0.7	4.01×10^{-3}	3.66×10^{-3}	3.46×10^{-3}	9.49×10^{-6}	9.12×10^{-8}	5.01×10^{-3}
0.9	1.57×10^{-3}	1.99×10^{-3}	1.26×10^{-3}	7.97×10^{-6}	6.34×10^{-9}	1.68×10^{-4}
CPU	–	–	–	2.734	2.485	2.562

TABLE 9. The residual errors with $k = 2, \gamma = 0.5$ for different values α (Example 5.6).

ξ	$\alpha = \frac{1}{4}$	$\alpha = \frac{1}{3}$	$\alpha = \frac{1}{2}$	$\alpha = \frac{3}{4}$	$\alpha = 1$
0.2	1.26×10^{-6}	2.40×10^{-7}	1.36×10^{-7}	1.98×10^{-5}	1.10×10^{-3}
0.4	3.82×10^{-6}	1.07×10^{-6}	1.09×10^{-6}	1.79×10^{-4}	2.55×10^{-2}
0.6	1.42×10^{-2}	2.39×10^{-3}	5.87×10^{-4}	3.55×10^{-3}	1.84×10^{-2}
0.8	6.63×10^{-3}	2.76×10^{-4}	9.18×10^{-4}	4.03×10^{-3}	2.84×10^{-2}
0.9	7.53×10^{-3}	8.33×10^{-4}	2.65×10^{-4}	1.11×10^{-3}	9.11×10^{-4}
CPU	3.641	3.375	2.485	3.532	3.312

TABLE 10. Numerical results with $k = 2, M = 11, \alpha = \frac{1}{2}$ (Example 5.6).

ξ	$\gamma = 0.25$	$\gamma = 0.5$	$\gamma = 0.75$
0.1	0.0422747343	0.0491353380	0.0707582268
0.2	0.1341864518	0.145604352	0.1775820988
0.3	0.2560367953	0.2621261275	0.3079749500
0.4	0.3980377198	0.4039046840	0.4577165762
0.6	0.7334084470	0.7375340296	0.8097405303
0.7	0.9339670628	0.9287239102	1.0136486495
0.8	1.1680772939	1.1398904957	1.2411533772
0.9	1.4494333080	1.3769096848	1.4989651939

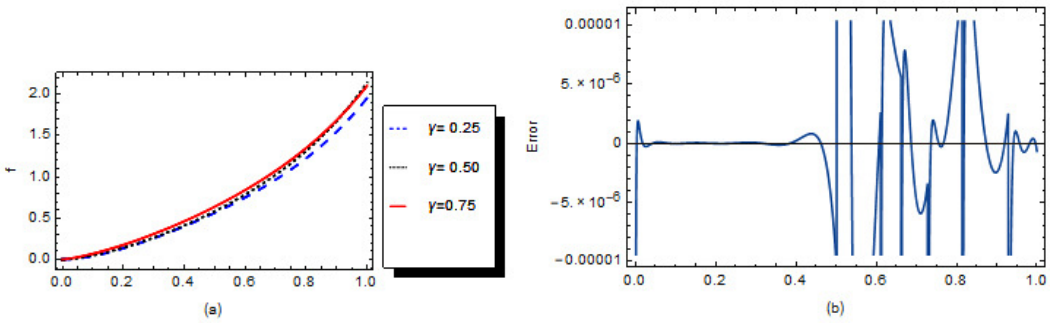

FIGURE 7. (a): Numerical solutions for diverse quantities of γ, (b): residual error for $\gamma = 0.5$ with $k = 2, M = 10, \alpha = \frac{1}{2}$ (Example 5.6).

Example 5.7. Let's consider the SFIDE given by [43]

$$\begin{cases} D^{\gamma} f(\xi) = \frac{\Gamma(3)\xi^{2-\gamma}}{\Gamma(3-\gamma)} - \frac{\xi^4 \sin(\xi)}{4} + \int_0^{\xi} \sin(\xi)\tau^2 f(\tau) d\tau + \int_0^{\xi} \tau e^{\xi} f(\tau) dB(\tau), \quad 0 \leq \tau, \quad \xi \leq 1, \\ f(0) = 0. \end{cases} \tag{5.11}$$

Table 11 compares the residual errors of the proposed technique for $k = 2, M = 11, \alpha = \frac{2}{3}$ with the shifted Legendre polynomial method with$N = 15$. Moreover, the residual errors and the CPU time obtained via the current strategy with $k = 2, \gamma = \alpha = 0.5$ for diverse quantities M are presented in Table 12. Numerical results with $k = 2, M = 11, \alpha = \frac{2}{3}$ and $\gamma = 0.25, 0.5, 0.75$ are given in Table 13. Also, the numerical results and the residual error for diverse values of γ with $k = 2$, $M = 10$, and $\alpha = \frac{2}{3}$ are displayed in Figure 8.

TABLE 11. The residual errors with $k = 2$, $\alpha = \frac{2}{3}$ (Example 5.7).

ξ	*Legendre polynomials method* $N = 15$			*Proposed strategy* $M = 11$		
	$\gamma = 0.25$	$\gamma = 0.5$	$\gamma = 0.75$	$\gamma = 0.25$	$\gamma = 0.5$	$\gamma = 0.75$
0.1	1.85×10^{-5}	1.76×10^{-4}	4.94×10^{-4}	6.21×10^{-9}	1.39×10^{-8}	2.56×10^{-8}
0.3	5.17×10^{-4}	3.94×10^{-4}	2.26×10^{-4}	4.34×10^{-8}	7.37×10^{-8}	1.29×10^{-7}
0.7	2.81×10^{-3}	2.92×10^{-3}	3.02×10^{-3}	1.33×10^{-4}	5.62×10^{-7}	2.24×10^{-7}
0.9	1.34×10^{-3}	1.34×10^{-3}	1.31×10^{-3}	3.76×10^{-6}	2.31×10^{-7}	6.47×10^{-7}
CPU	–	–	–	10.156	9.500	9.313

TABLE 12. The residual errors with $k = 2$, $\gamma = \alpha = 0.5$ for diverse quantities of M (Example 5.7).

ξ	$M = 6$	$M = 8$	$M = 9$	$M = 11$
0.2	5.85×10^{-6}	6.77×10^{-7}	1.65×10^{-8}	8.94×10^{-10}
0.4	1.20×10^{-4}	9.02×10^{-6}	2.08×10^{-7}	7.20×10^{-9}
0.6	1.98×10^{-2}	1.25×10^{-2}	3.45×10^{-5}	7.92×10^{-6}
0.8	1.62×10^{-3}	4.42×10^{-2}	1.27×10^{-4}	9.14×10^{-7}
CPU	1.094	3.672	6.266	7.578

TABLE 13. Numerical results with $k = 2, M = 11$, and $\alpha = \frac{2}{3}$ (Example 5.7).

ξ	$\gamma = 0.25$	$\gamma = 0.5$	$\gamma = 0.75$
0.1	0.0029748274	0.0036997412	0.0058228173
0.3	0.0528690758	0.0545356082	0.0676801756
0.7	0.4362363016	0.4060712777	0.4477611591
0.9	0.8545399486	0.7220298467	0.8093365430

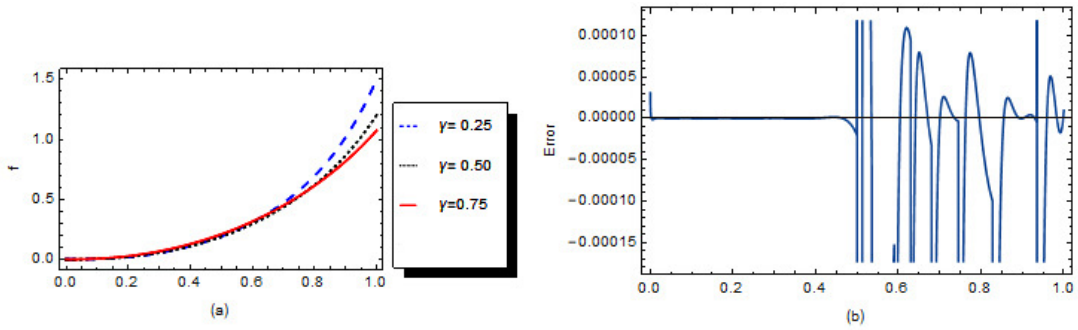

FIGURE 8. (a): Approximate solutions for various values of γ, (b): residual error for $\gamma = 0.5$ with $k = 2, M = 10, \alpha = \frac{2}{3}$ (Example 5.7).

Example 5.8. Let's consider the SFIDE given by [43]

$$\begin{cases} D^{\frac{1}{2}} f(\xi) + f(\xi) = \xi^2 + \frac{2\xi^{1.5}}{\Gamma(2.5)} + \int_0^\xi \tau dB(\tau), \quad 0 \le \tau, \xi \le 1, \\ f(0) = 0. \end{cases} \tag{5.12}$$

Table 14 presents the residual errors and computational times with $k = 2, \alpha = 0.5$ for different values of M. Also, Table 15 lists the residual errors with $k = 2, M = 11, \gamma = 0.5$, and various values α. These tables demonstrate the influence of parameters M and α.

TABLE 14. The residual errors with $k = 2, \alpha = 0.5$ for diverse cases of M (Example 5.8).

ξ	$M = 8$	$M = 9$	$M = 10$	$M = 11$
0.2	1.57×10^{-7}	1.95×10^{-8}	1.82×10^{-8}	1.36×10^{-11}
0.4	2.24×10^{-6}	2.51×10^{-7}	1.23×10^{-7}	8.60×10^{-10}
0.6	5.21×10^{-6}	4.57×10^{-6}	8.57×10^{-7}	3.02×10^{-9}
0.8	9.41×10^{-9}	4.65×10^{-9}	8.79×10^{-10}	1.53×10^{-12}
CPU	0.285	0.328	0.344	0.360

Applications in the physics.

Example 5.9. Let's examine the Linear pendulum problem given by [43]

$$\begin{cases} f_1(\xi) = \frac{\pi}{3} + \int_0^\xi f_2(\tau) d\tau, \\ f_2(\xi) = 1 - \int_0^\xi f_1(\tau) d\tau + \int_0^\xi (\gamma - \alpha f_2(\tau) - \beta f_1(\tau)) dB(\tau). \end{cases} \tag{5.13}$$

The absolute errors for the stochastic damping oscillator in the phase space with $\alpha = \frac{1}{10}, \gamma = \beta = 0$ and $T = 3\pi$ are listed in Table 16.

TABLE 15. The residual errors with $k = 2, \gamma = 0.5$ for various values of α (Example 5.8).

ξ	$\alpha = \frac{1}{4}$	$\alpha = \frac{1}{3}$	$\alpha = \frac{1}{2}$	$\alpha = \frac{3}{4}$	$\alpha = 1$
0.2	5.65×10^{-10}	2.34×10^{-9}	1.36×10^{-11}	1.33×10^{-8}	7.26×10^{-6}
0.4	4.30×10^{-9}	9.48×10^{-9}	8.60×10^{-10}	1.76×10^{-7}	2.55×10^{-4}
0.6	1.63×10^{-2}	8.12×10^{-8}	3.02×10^{-9}	8.43×10^{-8}	1.19×10^{-11}
0.8	2.67×10^{-3}	7.28×10^{-11}	1.53×10^{-12}	8.33×10^{-11}	9.06×10^{-14}

TABLE 16. The absolute errors with $\alpha = \frac{1}{10}, \gamma = \beta = 0$ and $T = 3\pi, k = 2$ (Example 5.9).

	$\xi = 0$	$\xi = \frac{\pi}{2}$	$\xi = \pi$	$\xi = 2\pi$	$\xi = \frac{5\pi}{2}$
Absolute error $(f_1(\xi))$					
$(M = 4)$	2.31×10^{-2}	2.98×10^{-1}	7.01×10^{-1}	3.05×10^{-2}	6.01×10^{-1}
$(M = 8)$	1.00×10^{-2}	4.05×10^{-2}	7.58×10^{-2}	7.97×10^{-3}	2.49×10^{-1}
Absolute error $(f_2(\xi))$					
$(M = 4)$	4.62×10^{-1}	9.10×10^{-1}	2.45×10^{-1}	8.30×10^{-1}	5.00×10^{-1}
$(M = 8)$	2.41×10^{-2}	4.43×10^{-3}	1.23×10^{-1}	8.65×10^{-2}	6.24×10^{-1}

6. Conclusion

A novel numerical technique based on the FGWs, inverse hyperbolic functions, and collocation strategy was introduced for obtaining numerical solutions of SFIDEs and IVIEs.Initially, we derived an approximation for the Caputo fractional derivative using the Laplace transform method, thereby converting fractional-order stochastic equations into integer-order ones. The solution was then approximated via a combination of FGWs and inverse hyperbolic functions. A system of algebraic equations was derived using the GLQR and the collocation approach.This resulting system was efficiently solved using Newton's iterative method. The reliability and precision of the proposed approach were demonstrated on several numerical examples.

Acknowledgements

We express our sincere thanks to the anonymous referees for valuable suggestions that improved the paper.

Data availability statement

Data will be made available on reasonable request.

Declaration of Competing Interest

The authors wish to confirm that there are no known conflicts of interest associated with this publication and there has been no significant financial support for this work that could have influenced its outcome.

Authors contributions

All authors contributed equally and significantly in writing this article. All authors read and approved the final manuscript.

References

[1] J. A. Appley, S. Devin, and D. W. Reynolds, *Almost sure convergence of solutions of linear stochastic Volterra equations to nonequilibrium limits*, J. Integ. Equ. Appl., *19*(4) (2007), 405–437.

[2] M. Asgari, *Block pulse approximation of fractional stochastic integro-differential equation*, Commun. Numer. Anal., *2014* (2014), 1–7.

[3] A. A. Badr and H. S. El-Hoety, *Monte-Carlo Galerkin approximation of fractional stochastic integro-differential equation*, Math. Probl. Eng., *2012*(1) (2012), 709106.

[4] M. A. Berger and V. J. Mizel, *Volterra equations with Itô integrals*, I, J. Integ. Equ., *2* (1980), 187–245.

[5] P. A. Cioica and S. Dahlke, *Spatial Besov regularity for semilinear stochastic partial differential equations on bounded Lipschitz domains*, Int. J. Comput. Math., *89*(18) (2012), 2443–2459.

[6] I. Daubechies, *Orthonormal bases of compactly supported wavelets*, Comm. Pure Appl. Math., *41*(7) (1988), 909–996.

[7] H. Dehestani, Y. Ordokhani, and M. Razzaghi, *A numerical technique for solving various kinds of fractional partial differential equations via Genocchi hybrid functions*, RACSAM, *113* (2019), 3297–3321.

[8] H. Dehestani, Y. Ordokhani, and M. Razzaghi, *Fractional-order Genocchi-Petrov-Galerkin method for solving time-space fractional Fokker-Planck equations arising from the physical phenomenon*, Inter. J. Appl. Comput. Math., *6*(4) (2020), 1–31.

[9] N. Engheta, *On fractional calculus and fractional multipoles in electromagnetism*, IEEE Trans. Antennas Propag. *44*(4) (1996), 554.

[10] S. Fomin, V. Chugunov, and T. Hashida, *Application of fractional differential equations for modeling the anomalous diffusion of contaminant from fracture into porous rock matrix with bordering alteration zone*, Transp. Porous. Med., *81* (2010), 187–205.

[11] R. M. Ganji, H. Jafari, and S. Nemati, *A new approach for solving integro-differential equations of variable order*, J. Comput. Appl. Math., *379* (2020), 112946.

[12] M. H. Heydari, M. R. Hooshmandasl, C. Cattani, and F. M. Maalek Ghaini, *An efficient computational method for solving nonlinear stochastic Itô integral equations: Application for stochastic problems in physics*, J. Comput. Phys., *283* (2015), 148–168.

[13] M. H. Heydari, M. R. Hooshmandasl, F. M. Maalek Ghaini, and C. Cattani, *A computational method for solving stochastic Itô-Volterra integral equations based on stochastic operational matrix for generalized hat basis functions*, J. Comput. Phys., *270* (2014), 402–415.

[14] D. J. Higham, *An algorithmic introduction to numerical simulation of stochastic differential equations*, SIAM Rev., *43*(3) (2001), 525–546.

[15] M. Khodabin, K. Maleknejad, and T. Damercheli, *Approximate solution of the stochastic Volterra integral equations via expansion method*, Int. J. Indus. Math., *6*(1) (2014), 41–48.

[16] M. Khodabin, K. Maleknejad, and F. Hosseini Shekarabi, *Application of triangular functions to numerical solution of stochastic Volterra integral equations*, IAENG Int. J. Appl. Math., *43*(1) (2013), 1–9.

[17] M. Khodabin, K. Maleknejad, M. Rostami, and M. Nouri, *Interpolation solution in generalized stochastic exponential population growth model*, Appl. Math. Modell., *36*(3) (2012), 1023–1033.

[18] R. C. Koeller, *Applications of fractional calculus to the theory of viscoelasticity*, J. Appl. Mech., *51*(2) (1984), 299–307.

[19] S. Mallat, *A theory of multiresolution signal decomposition: the wavelet representation*, IEEE Trans. Pattern Anal. Mach. Intell., *11*(7) (1989), 674–693.

[20] F. Mirzaee and E. Hadadiyan, *A collocation technique for solving nonlinear stochastic Itô-Volterra integral equations*, Appl. Math. Comput., *247* (2014), 1011–1020.

[21] F. Mirzaee and N. Samadyar, *Application of orthonormal Bernstein polynomials to construct a efficient scheme for solving fractional stochastic integro-differential equation*, Optik, *132* (2017), 262–273.

[22] F. Mirzaee, N. Samadyar, and S. F. Hoseini, *Euler polynomial solutions of nonlinear stochastic Itô-Volterra integral equations*, J. Comput. Appl. Math., *330*(1) (2018), 574–585.

[23] F. Mohammadi, *A wavelet-based computational method for solving stochastic Itô-Volterra integral equations*, J. Comput. Phys., *298* (2015), 254–265.

[24] F. Mohammadi, *Wavelet Galerkin method for solving stochastic fractional differential equations*, J. Fract. Calc. Appl., *7*(1) (2016), 73–86.

[25] B. Oksendal, *Stochastic Differential Equations*, An Introduction with Applications, Fifth Edition, Springer-Verlag, New York, (1998).

[26] K. B. Oldham, *Fractional differential equations in electrochemistry*, Adv. Eng. Softw., *41* (2010), 9–12.
[27] K. Parand and M. Nikarya, *Application of Bessel functions and spectral methods for solving differential and integro-differential equations of the fractional order*, Appl. Math. Model., *38* (2014), 4137–4147.
[28] P. Rahimkhani, *A numerical method for Ψ-fractional integro-differential equations by Bell polynomials*, Appl. Numer. Math., *207* (2025), 2447–253.
[29] P. Rahimkhani, *Numerical solution of nonlinear stochastic differential equations with fractional Brownian motion using fractional-order Genocchi deep neural networks*, Commun. Nonlinear Sci. Numer. Simul., *126* (2023), 107466.
[30] P. Rahimkhani and M. H. Heydari, *Numerical investigation of ψ-fractional differential equations using wavelets neural networks*, Comput. Appl. Math., *44*(1) (2025), 1–18.
[31] P. Rahimkhani and Y. Ordokhani, *Approximate solution of nonlinear fractional integro-differential equations using fractional alternative Legendre functions*, J. Comput. Appl. Math., *365* (2020), 112365.
[32] P. Rahimkhani and Y. Ordokhani, *Numerical investigation of distributed-order fractional optimal control problems via Bernstein wavelets*, Optim. Control Appl. Methods, *42*(1) (2021), 355–373.
[33] P. Rahimkhani, Y. Ordokhani, and E. Babolian, *A new operational matrix based on Bernoulli wavelets for solving fractional delay differential equations*, Numer. Algorithms, *74* (2017), 223–245.
[34] P. Rahimkhani, Y. Ordokhani, and E. Babolian, *Fractional-order Bernoulli functions and their applications in solving fractional Fredholem-Volterra integro-differential equations*, Appl. Nume. Math., *122* (2017), 66–81.
[35] P. Rahimkhani, Y. Ordokhani, and E. Babolian, *Müntz-Legendre wavelet operational matrix of fractional-order integration and its applications for solving the fractional pantograph differential equations*, Numer. Algorithms, *77*(4) (2018), 1283–1305.
[36] P. Rahimkhani, Y. Ordokhani, and P. M. Lima, *An improved composite collocation method for distributed-order fractional differential equations based on fractional Chelyshkov wavelets*, Appl. Numer. Math., *145* (2019), 1–27.
[37] J. Ren, Z. Sun, and W. Dai, *New approximations for solving the Caputo-type fractional partial differential equations*, Appl. Math. Model., *40*(4) (2016), 2625–2636.
[38] S. Sabermahani and Y. Ordokhani, *A new operational matrix of Müntz-Legendre polynomials and Petrov-Galerkin method for solving fractional Volterra-Fredholm integro-differential equations*, Comput. Methods Differ. Equ., *8* (2020), 408–423.
[39] S. Sabermahani and Y. Ordokhani, *Fibonacci wavelets and Galerkin method to investigate fractional optimal control problems with bibliometric analysis*, J. Vib. Control., *27*(15-16) (2021), 1778–1792.
[40] S. Sabermahani, Y. Ordokhani, and P. Rahimkhani, *Spectral methods for solving integro-differential equations and bibiliometric analysis*, Topics in Integral and Integro-Differential Equations: Theory and Applications, (2021), 169–214.
[41] Sh. Sharma, R. K. Pandey, and K. Kumar, *Galerkin and collocation methods for weakly singular fractional integro-differential equations*, Iran. J. Sci. Technol. Trans. Sci., *43* (2019), 1649–1656.
[42] J. Stoer and R. Bulirsch, *Introduction to Numerical Analysis*, 2nd edn, Springer, Berlin, (2002).
[43] Z. Taheri, Sh. Javadi, and E. Babolian, *Numerical solution of stochastic fractional integro-differential equation by the spectral collocation method*, J. Comput. Appl. Math., *321* (2017), 336–347.
[44] Y. H. X. Zhang and B. Tang, *Homotopy analysis method for higher-order fractional integro-differential equations*, Comput. Math. Appl., *62* (2011), 3194–3203.